BBA - Molecular Basis of Disease 1865 (2019) 218–229

Contents lists available at ScienceDirect

BBA - Molecular Basis of Disease

journal homepage: www.elsevier.com/locate/bbadis

Galectin-1 attenuates cardiomyocyte hypertrophy through splice-variant specific modulation of $Ca_V1.2$ calcium channel

Jia Fan[a,1], Wenyong Fan[a,1,2], Jianzhen Lei[a], Yingying Zhou[a], Hongfei Xu[b], Isha Kapoor[c], Guoqing Zhu[a], Juejin Wang[a,d,*]

[a] Key Laboratory of Cardiovascular Disease and Molecular Intervention, Department of Physiology, Nanjing Medical University, Nanjing, Jiangsu 211166, China
[b] Department of Physiology, Nanjing Medical University, Nanjing, Jiangsu 211166, China
[c] Department of Cancer Biology, Lerner Research Institute, Cleveland Clinic, Cleveland, OH 44195, USA
[d] Key Laboratory of Human Functional Genomics of Jiangsu Province, Nanjing Medical University, Nanjing, Jiangsu 211166, China

ARTICLE INFO

Keywords:
Galectin-1
$Ca_V1.2$ calcium channel
Alternative splicing
Cardiomyocyte hypertrophy

ABSTRACT

Pressure overload-induced cardiac hypertrophy occurs in response to chronic blood pressure increase, and dysfunction of $Ca_V1.2$ calcium channel involves in cardiac hypertrophic processes by perturbing intracellular calcium concentration ($[Ca^{2+}]_i$) and calcium-dependent signaling. As a carbohydrate-binding protein, galectin-1 (Gal-1) is found to bind with $Ca_V1.2$ channel, which regulates vascular $Ca_V1.2$ channel functions and blood pressure. However, the potential roles of Gal-1 in cardiac $Ca_V1.2$ channel ($Ca_V1.2_{CM}$) and cardiomyocyte hypertrophy remain elusive. By whole-cell patch clamp, we find Gal-1 decreases the $I_{Ca,L}$ with or without isoproterenol (ISO) application by reducing the channel membrane expression in neonatal rat ventricular myocytes (NRVMs). Moreover, Gal-1 could inhibit the current densities of $Ca_V1.2_{CM}$ by an alternative exon 9*-dependent manner in heterologously expressed HEK293 cells. Of significance, overexpression of Gal-1 diminishes ISO or KCl-induced $[Ca^{2+}]_i$ elevation and attenuates ISO-induced hypertrophy in NRVMs. Mechanistically, Gal-1 decreases the ISO or Bay K8644-induced phosphorylation of intracellular calcium-dependent signaling proteins δCaMKII and HDAC4, and inhibits ISO-triggered translocation of HDAC4 in NRVMs. Pathologically, we observe that the expressions of Gal-1 and $Ca_V1.2_{E9*}$ channels are synchronously increased in rat hypertrophic cardiomyocytes and hearts. Taken together, our study indicates that Gal-1 reduces the channel membrane expression to inhibit the currents of $Ca_V1.2_{CM}$ in a splice-variant specific manner, which diminishes $[Ca^{2+}]_i$ elevation, and attenuates cardiomyocyte hypertrophy by inhibiting the phosphorylation of δCaMKII and HDAC4. Furthermore, our work suggests that dysregulated Gal-1 and $Ca_V1.2$ alternative exon 9* might be attributed to the pathological processes of cardiac hypertrophy, and provides a potential anti-hypertrophic target in the heart.

1. Introduction

Cardiac hypertrophy could be attributed to the increased afterload pressure of left ventricles and upregulated sympathetic activity which excites β-adrenergic receptors on heart [1]. As an excitation-contraction coupling factor, intracellular Ca^{2+} is closely associated with cardiac hypertrophy, it mediates cellular functions by affecting the intracellular Ca^{2+}-dependent kinases to regulate hypertrophic genes expression [2]. Specifically, Ca^{2+}/calmodulin-dependent protein kinase II (CaMKII), a serine/threonine kinase, is regulated by Ca^{2+}/calmodulin complex. CaMKII can phosphorylate histone deacetylases 4 (HDAC4), resulting into upregulation of hypertrophic related fetal genes' transcription, such as *Nppa* (ANP), *Nppb* (BNP) and *Myh7* (β-MHC) [3].

Abbreviations: AID, α-interaction domain; CaMKII, Ca^{2+}/calmodulin-dependent protein kinase II; $Ca_V1.2_{CM}$, cardiac $Ca_V1.2$ channel; $[Ca^{2+}]_i$, intracellular calcium concentration; CICR, calcium-induced calcium release; DTZ, diltiazem; ER, endoplasmic reticulum; Gal-1, galectin-1; HDAC4, histone deacetylases 4; HEK293, human embryonic kidney-293; ISO, isoproterenol; LTCC, L-type calcium channel; IVS, interventricular septum dimension; LVPW, left ventricular posterior wall; NRVM, neonatal rat ventricular myocyte; PKA, protein kinase A; SHR, spontaneously hypertensive rat; TAC, transverse aortic restriction; VSMC, vascular smooth muscle cell; WKY, Wistar-Kyoto rat

* Corresponding author at: Department of Physiology, Nanjing Medical University, 101 Longmian Avenue, Nanjing, Jiangsu 211166, China.
E-mail address: juejinwang@njmu.edu.cn (J. Wang).
[1] These authors contributed equally to this work.
[2] Present address: Department of Physiology and Biophysics, School of Life Sciences, Fudan University, Shanghai 200438, China.

https://doi.org/10.1016/j.bbadis.2018.08.016
Received 28 April 2018; Received in revised form 17 July 2018; Accepted 14 August 2018
Available online 16 August 2018

In mammalian cardiomyocyte, Ca^{2+} influx from activated $Ca_V1.2$ L-type calcium channel (LTCC) triggers the increase of intracellular Ca^{2+} concentration ($[Ca^{2+}]_i$). This increase of $[Ca^{2+}]_i$ is mediated by calcium-induced calcium release (CICR), that leads to contraction of myofilaments and regulation of downstream genes expression by a cascade of signaling pathways [4]. Dysfunctions of cardiac $Ca_V1.2$ calcium channel are found in cardiac hypertrophy, this abnormal $Ca_V1.2$ channels perturb the homeostasis of intracellular calcium signaling [5–8]. Though it remains intriguing [9], calcium channel blockers are thought to have some beneficial effects on the ventricular hypertrophy in murine models [10,11]. These imply that the intracellular modulators of $Ca_V1.2$ channel might have some roles in cardiac hypertrophy.

Pre-mRNA alternative splicing, as one of post-transcriptional modulation mechanisms, optimizes the functions of $Ca_V1.2$ calcium channels. Human and rat $Ca_V1.2$ α_{1C} are identified to have many alternatively spliced exons [12,13]. Of which, the alternative exon 9*, located at I-II loop of $Ca_V1.2$ α_{1C} subunit, plays crucial role in the electrophysiological functions of $Ca_V1.2$ calcium channels [14–18]. The expression of $Ca_V1.2$ channels with alternative exon 9* ($Ca_V1.2_{E9*}$) is known to be deregulated under cardiovascular pathological conditions [19–22]. However, the expression of $Ca_V1.2_{E9*}$ channel and its potential roles in cardiac hypertrophy are not fully understood.

Galectins are a family of carbohydrate-binding proteins which exhibit strong affinity for β-galactosides [23], they are shown to play diverse roles in different cardiac diseases [24]. As one member of galectin family, galectin-1 (Gal-1) was initially recognized to regulate immune responses and cancer progression [25,26]. However, it could regulate other cellular processes, like differentiation, proliferation and migration of vascular smooth muscle cells (VSMCs) [27]. Indeed, Gal-1 could directly bind to I-II loop of $Ca_V1.2$ calcium channel, which leads to the degradation of $Ca_V1.2$ channels [28]. This splice-variant specific binding induced a decrease in $Ca_V1.2$ calcium channel currents, which regulated vascular constriction and blood pressure [18,28]. Of significance, Gal-1 was reported to play potential roles in ventricular remodeling [29], and the expression of Gal-1 was increased in mouse and human acute myocardial infarction [30]. However, whether and how Gal-1 affects the function of cardiac $Ca_V1.2$ calcium channel and cardiomyocyte hypertrophy are largely unknown.

In this work, we uncovered that Gal-1 could attenuate cardiomyocyte hypertrophy via LTCC-δCaMKII-HDAC4 signaling pathway in a splice-variant specific manner, and the expressions of Gal-1 and $Ca_V1.2$ exon 9* are synchronously increased in cardiac hypertrophy. Therefore, our findings elucidated the effects of the interaction between Gal-1 and $Ca_V1.2$ channels on cardiomyocyte hypertrophy, which provided a promising anti-hypertrophic target in the heart.

2. Materials and methods

2.1. Animals

All animals were treated ethically in according to the Guide for the Care and Use of Laboratory Animals, and animal protocol was approved by Institutional Animal Care and Use Committee of Nanjing Medical University (Nanjing, China). Afterload-induced cardiac hypertrophy was conducted by transverse aortic restriction (TAC) in adult male Sprague-Dawley (SD) rats as previously described [31,32]. Shortly, the rats (~200–250 g body weight) were anesthetized by 2% isoflurane in O_2 and placed in the supine position and midline cervical incision was exposed to trachea. After endotracheal intubation, the cannula was connected to a volume-cycled rodent ventilator (Harvard Apparatus, Holliston, Massachusetts, USA). 27-gauge needle was ligated with transverse aorta, which positioned between the right and left carotid arteries and removed after placement of the ligature. The rats were monitored for 10–14 days after surgery. Spontaneously hypertensive rats (SHR) and non-hypertensive Wistar-Kyoto (WKY) rats were purchased from Vital River (Beijing, China). All rats were maintained in individually ventilated cages with an artificial 12-hour dark-light cycle, with free access to standard chow and drinking water. Approximately, 60 rats were used in this study. Systolic blood pressure of rats was measured by tail cuff plethysmography (PowerLab, ADInstruments, Bella Vista, New South Wales, Australia).

2.2. Echocardiography

Transthoracic echocardiographic measurements were performed using a Vevo 2100 ultrasound machine (VisualSonics, Canada) and a 14 MHz transducer placed in a parasternal short-axis view position in rats. Anesthetized rats (2% isoflurane in O_2, 1 L/min) were maintained at 37 °C with a heating pad. M-mode tracings were used to measure interventricular septum dimension (IVS), left ventricular posterior wall dimension (LVPW), and left ventricular internal dimension (LVID). The teichholz formula was used to calculate fractional shortening (FS) and left ventricular ejection fraction (LVEF), as described previously [33]. All measurements were averaged over six consecutive cardiac cycles and performed by the investigator who was blinded with respect to the identity of the tracings.

2.3. Primary neonatal rat ventricular cardiomyocytes isolation

Neonatal rat ventricular myocytes (NRVMs) were isolated from 1 to 2-day-old SD rats' heart by enzymatic digestion [34,35]. Briefly, beating hearts were harvested from < 48 h-old SD rats and immediately placed into cooled Ca^{2+} and Mg^{2+} free Hanks balance salt solution (HBSS). The hearts were gently washed with HBSS and non-heart tissue was removed under a stereomicroscopy. Heart tissues were then cut into small pieces with a curved scissors in a sterile centrifuge tube. After that, cells were digested by an enzyme cocktail containing 0.06% pancreatin (Sigma-Aldrich, USA) and 0.04% type II collagenase (Sigma-Aldrich) dissolved in Ca^{2+}/Mg^{2+} free HBSS at 37 °C. Fibroblasts were removed from the cell suspension by 1 h differential plating and NRVMs were cultured in DMEM medium (Gibco, Thermo Fisher Scientific, USA) containing 10% fetal bovine serum (FBS), penicillin (100 U/mL, Gibco), streptomycin (100 μg/mL, Gibco), HEPES (25 mmol/L) and glutamine (2 mmol/L) in the 5% CO_2 incubator. Culture medium was changed to DMEM with 2% FBS after the cells had attached to the culture plate and beat rhythmically. NRVMs were incubated with 1 μmol/L isoproterenol (ISO) (Sigma-Aldrich) for 48 h to induce stable hypertrophy [36].

2.4. DNA constructs

The human $Ca_V1.2_{CM}$ construct ($Ca_V1.2_{CM\Delta E9*}$), as most abundant isoform expressed in cardiac myocyte [15,18], excludes alternative exon 9*, but contains alternative exon 1a, exon 8a, exon 32 and exon 33. The construct of $Ca_V1.2_{CME9*}$ was generated by replacing a PCR fragment containing exon 9* using *Cla*I and *Sgr*AI sites. The construct was validated by DNA sequencing. Gal-1 expression plasmids were generated by using pIRES$_2$-DsRed or pcDNA3.1 expression vector as described previously [18].

2.5. Cell culture and transfection

Human embryonic kidney-293 (HEK293) cells were cultured in DMEM medium supplemented with 10% FBS and 1% penicillin and streptomycin and maintained in 5% CO_2 incubator at 37 °C. For transfection, HEK293 cells were seeded in petri dish containing cover slips and grown overnight, and then the plasmids expressing human $Ca_V1.2$ calcium channels were transfected into HEK293 cells by calcium phosphate method. Briefly, in 35 mm petri dish, 1.7 μg human $Ca_V1.2$ α_{1C} plasmids together with 1.25 μg of human β_{2a}, 1.25 μg of $\alpha_2\delta_1$, and 0.25 μg of TAG (T antigen) plasmids were transiently co-transfected with 2 μg Gal-1 expression plasmids into HEK293 cells. For NRVMs

transfection, the cells were cultured in 6-well plates or 35 mm petri dishes containing cover slips, 2 μg of Gal-1 expression plasmids or empty vectors were transfected by Lipofectamine 3000 (Invitrogen, Thermo Fisher Scientific, USA) according to the manufacturer's protocol. For knocking down Gal-1 expression, 2 μg pooled short hairpin RNAs (shRNAs) targeting with different regions of rat Gal-1 mRNA (NM_019904) (GeneChem, Shanghai, China) were transfected into NRVMs by Lipofectamine 3000. The sequences of shRNAs were listed in Table S1.

2.6. RNA extraction and RT-PCR analysis

Total RNA was extracted from rat left ventricular tissues or NRVMs by using Trizol reagent (Invitrogen) following the manufacture's protocol. Total RNA (1 μg) was reversely transcribed to cDNA by using Prime Script RT Master Mix kit (Takara, Japan). Semi-quantitative PCR was carried out with DreamTaq Green PCR Master Mix (Invitrogen). PCR products were separated on a 2% agarose gel. Quantitative real-time PCR (qPCR) was performed using SYBR Green Master Mix (Takara, Japan) on StepOne Plus real-time PCR system (Applied Biosystems, Thermo Fisher Scientific, USA). Primers used in this study were listed in Table S2.

2.7. Extraction of membrane protein

Membrane protein preparation steps were carried out on ice following previously described protocol [18,22]. Briefly, cells were collected and lysated in ice-cold lysis buffer (20 mM Tris-HCl, 150 mM $NaCl_2$, pH 7.4, protease inhibitor added) after different treatment. First, the lysate was centrifuged for 10 min at 1000*g*, then the supernatant containing membranes were collected and centrifuged at 90,000*g* for 40 min. The supernatant was collected as cytosol protein, and the final pellet was resuspended in lysis buffer as membrane protein for later analysis.

2.8. Western blotting

Total proteins were extracted from cultured NRVMs or tissues by RIPA lysis buffer with protease inhibitor cocktail or phosphatase inhibitor cocktail (Selleckchem, China). Protein concentrations were determined by Bradford assay (Bio-Rad, USA), and equal amounts of total proteins were separated on SDS-PAGE and transferred to PVDF membrane. After blocking, PVDF membranes were incubated with primary antibodies overnight at 4 °C or 1 h at room temperature, followed by incubating with HRP-linked secondary antibody (Sigma-Aldrich, 1:10,000 dilution) for 1 h at room temperature. The protein bands were visualized with Immubilon Western Chemiluminescent HRP Substrate Kit (Merck Millipore, German).

2.9. Immunofluorescence

Freshly isolated rat ventricles were fixed in 4% paraformaldehyde in PBS 2–4 h at 4 °C and then incubated in 20–30% sucrose in PBS overnight. The tissues were cryo-sectioned to 20 μm in thickness, the sections were blocked with 0.3% BSA and 0.1% Triton X-100 in PBS for 40 min at room temperature. NRVMs were fixed in 4% paraformaldehyde for 15 min and permeabilized for 30 min with PBS with 0.1% Triton X-100 and 0.3% BSA at 4 °C. The permeabilized tissues or cells were blocked with 0.3% BSA for another 30 min, and then incubated with different antibodies overnight at 4 °C. After that, the slides were incubated in Alexa 488 or Alexa 562-conjugated secondary antibodies (Molecular Probes, Thermo Fisher Scientific, USA) away from light for 1 h at room temperature. The images were collected on a Zeiss 710 Meta confocal microscope (Carl Zeiss, German), with a pinhole of 1.0 airy disc, using the Zeiss image acquisition software. All images were exported to Photoshop (Adobe, USA) for cropping and linear adjustment of contrast.

2.10. Whole-cell patch clamp recording

The external solution for recording HEK293 cells contained (in mM) 144 TEA-$MeSO_3$ (or 140 TEA-$MeSO_3$), 10 HEPES, 1.8 $CaCl_2$ (or 5 $BaCl_2$), pH was adjusted to 7.4 with CsOH and osmolarity to 300–310 mOsm with glucose. The internal solution (pipette solution) contained (in mM) 138 Cs-MeSO3, 5 CsCl, 0.5 EGTA, 10 HEPES, 1 $MgCl_2$, 2 mg/mL Mg-ATP, pH 7.3 (adjusted with CsOH). Glucose was used to adjust the osmolarities of solutions to between 290 and 300 mOsm. The external solution for recording NRVMs contained (in mM) 140 TEA-Cl, 10 HEPES, 1 $MgCl_2$, 5 $CaCl_2$, 10 glucose, pH 7.4, osmolarities 300–310 mOsm. The internal solution (pipette solution) contained (in mM) 130 CsCl, 5 EGTA, 1 $MgCl_2$, 10 HEPES, 2 Na_2ATP, 0.5 GTP, 10 glucose, pH 7.2, osmolarities 290–300 mOsm. Whole-cell currents obtained under voltage-clamp with an Axopatch 200B amplifier (Molecular Device, San Jose, California, USA), were filtered at 1–5 kHz and sampled at 5–50 kHz, and the series resistance was typically < 5 MΩ after $> 70\%$ compensation. The P/4 protocol was used to subtract online the leak and capacitive transients. Whole-cell recording of spontaneous action potentials of cardiomyocyte was carried out in the current-clamp mode. The extracellular bath contained (in mM): NaCl 137, KCl 5.4, $MgCl_2$ 1, NaH_2PO_4 0.33, HEPES 10, glucose 10, $CaCl_2$ 1.8, pH adjusted to 7.4 with NaOH. The pipette solution contained (in mM): potassium gluconate 123, NaCl 9, $MgCl_2$ 1.8, EGTA 0.9, HEPES 9, phosphocreatine 14, MgATP 4, pH adjusted to 7.2 with KOH.

$Ca_V1.2$ calcium channel currents were recorded using different pulse protocols as previously described [18,37]. Briefly, calcium channel currents were recorded by holding the cell at −90 or −70 mV (for HEK293 and NRVMs respectively) before stepping to various potentials from −50 to 50 mV over 900 ms, then the *I-V* curve was fitted with the equation: $I = G_{max}(V - E_{rev}) / (1 + \exp(V - V_{1/2})/k)$, where G_{max} is the maximum conductance, E_{rev} is the reversal potential, $V_{1/2}$ is the half-activation potential, and k is the slope rate. ON-gating charge (Q_{ON}) was measured by holding the cells at −90 mV before applying a 6 ms long pulse at reversal potential (V_{rev}) where no ionic inward and outward currents were observed. Q_{ON} currents were quantified by current integration over the first 2 ms of the test pulse to V_{rev}, and normalized to cell capacitance [18].

2.11. Measurement of cytosolic Ca^{2+} concentration

Cytosolic calcium concentration was measured using 4 μmol/L Fluo-4 AM (Molecular Probes) as previous description [38]. Briefly, NRVMs were bathed in Tyrode solution, containing (in mmol/L) 140 NaCl, 5.4 KCl, 1.8 $CaCl_2$, 1 $MgCl_2$, 10 HEPES and 10 glucose, pH was adjusted to 7.4 with NaOH. Cells were transferred to laminin-coated culture dishes on the stage of a confocal microscope (LSM 710, Carl Zeiss, German). Images were obtained by time series scanning mode and sampled at 1 fps, and fluorescence intensity was analyzed offline. In order to calibrate the fluorescence signals of intracellular Ca^{2+} indicator, we divided the changes in the fluorescent signal by the average resting fluorescence according to the formula: $\Delta[Ca^{2+}]_i = \Delta F/F_0 = (F - F_0) / F_0$, where F is the dye fluorescence at any given time and F_0 is the average fluorescence signal prior to an experimental manipulation [39].

2.12. Statistical analysis

Data are reported as mean ± S.E.M. n number refers to biological repeats. Statistical significance was analyzed using a Student's unpaired *t*-test or one-way ANOVA followed by a Newman-Keuls method for post hoc pair-wise multiple comparisons. A value of $P < 0.05$ was set as significant statistic difference.

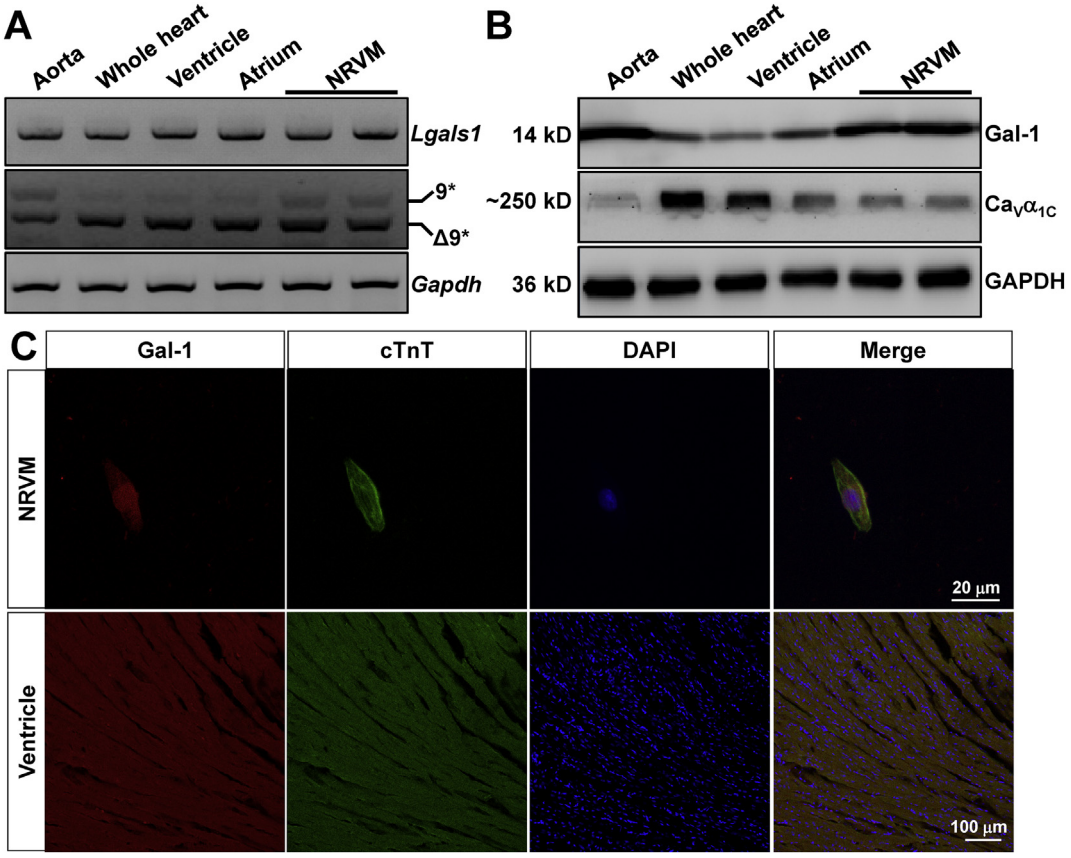

Fig. 1. Gal-1 and $Ca_V1.2$ channels with or without alternative exon 9* are expressed in rat heart. (A) PCR products were separated on 2% agarose gel. Rat aorta, whole heart, ventricle, atrium and isolated NRVMs contained the product of *Lgals1* (*Gal-1*) mRNA and $Ca_V1.2$ channels with (upper bands) or without exon 9* (lower bands). *Gapdh* mRNA was detected as loading control. (B) Gal-1 protein and $Ca_V1.2$ α_{1C} as detected by Western blotting were also observed in the rat aorta, heart tissues and isolated NRVMs, GAPDH protein was detected as internal control. (C) Immunofluorescence staining to determine the localization of Gal-1 in cardiomyocytes and cardiac muscle was carried out using anti-Gal-1 antibody (left panel, 1:100 dilution), and anti-cardiac troponin T (cTnT) antibody (middle panel, 1:100 dilution), the right panel shows the merged image.

3. Results

3.1. Gal-1 and $Ca_V1.2$ with or without alternative exon 9* are expressed in rat heart

Gal-1 has been reported to be expressed abundantly at vascular smooth muscle, whether Gal-1 is co-expressed with $Ca_V1.2_{E9*}$ or $Ca_V1.2_{\Delta E9*}$ channels in heart is unclear. To address this issue, we first used RT-PCR approach to determine that *Lgals1* (*Gal-1*) mRNA was expressed in aorta, adult hearts and isolated NRVMs from rats. By using specific primers, we detected the cardiac tissues expressed both $Ca_V1.2_{E9*}$ and $Ca_V1.2_{\Delta E9*}$ channels, but the NRVMs expressed more $Ca_V1.2_{E9*}$ channels than adult cardiac tissues (Fig. 1A). We also found that Gal-1 and $Ca_V1.2$ α_{1C} proteins were expressed in rat aorta, adult hearts and NRVMs by Western blotting (Fig. 1B). Interestingly, Gal-1's expression in neonatal cardiomyocytes is found to be more than adult cardiomyocytes (Fig. S1). Further, by using immunofluorescence staining, we confirmed Gal-1 was expressed in isolated NRVMs (Fig. 1C upper panel) and rat ventricular tissue (Fig. 1C lower panel), stained with cardiac troponin T. These indicated that Gal-1 and $Ca_V1.2$ alternative exon 9* in heart might play some roles in cardiac myocytes.

3.2. Gal-1 decreases the currents of cardiac $Ca_V1.2$ channel

Though Gal-1 is known to regulate the calcium currents in the VSMCs [18], its function on the cardiac $Ca_V1.2$ is unknown. To this end, NRVMs were transfected with Gal-1 expression plasmids, and post 48 h transfection, Western blotting revealed increased expression of Gal-1 (~2.5-folds) in comparison to vector-transfected NRVMs. Moreover, the expression of Gal-1 was also found to be increased ~2-folds in Gal-1-transfected cells when compared with vector-transfected cells upon application with ISO (Fig. 2A–B). Herein, overexpression of Gal-1 could inhibit the basal currents of $Ca_V1.2$ channel (Fig. 2C), and $Ca_V1.2$ calcium currents were also diminished by Gal-1 upon application with 1 μmol/L ISO in NRVMs (Fig. 2D). Furthermore, we detected the membrane expression of $Ca_V1.2$ channels in NRVMs (Fig. 2E), it is found that overexpression of Gal-1 could significantly reduce the surface expression level of $Ca_V1.2$ α_{1C} protein in non-treated and ISO-treated NRVMs, respectively (Fig. 2F). In contrast to overexpression of Gal-1, knockdown of Gal-1 in NRVMs potentiated the $I_{Ca,L}$ upon the application with ISO (Fig. S2A, B and D), though the basal $I_{Ca,L}$ remained unchanged (Fig. S2A–C). Thus, our results indicated that Gal-1 could directly inhibit basal and ISO-induced $Ca_V1.2$ currents in cardiomyocyte by reducing the membrane expression of $Ca_V1.2$ channels. As calcium ionic flow also involves in the formation of cardiac action potentials (APs), inhibition of $I_{Ca,L}$ by Gal-1 might affect the waveform of APs. As expected, we observed that Gal-1 overexpression could decrease the action potential duration after 70% replorization (APD_{70}) in NRVMs (Fig. S3A and D). However, maximal diastolic potential (Fig. S3B) and amplitude (Fig. S3C) of APs remained unchanged.

Gal-1 is known to regulate vascular $Ca_V1.2$ channel in an exon 9*-dependent manner [18], whether Gal-1 affects the cardiac $Ca_V1.2$ channel in same manner remains unclear. Here, we used $Ca_V1.2_{CM\Delta E9*}$, the major isoform expressed in the cardiac muscles without alternative exon 9* [15,18], to generate the $Ca_V1.2$ with inclusion of exon 9* ($Ca_V1.2_{CME9*}$). By whole-cell patch clamp, we found that Gal-1 did not

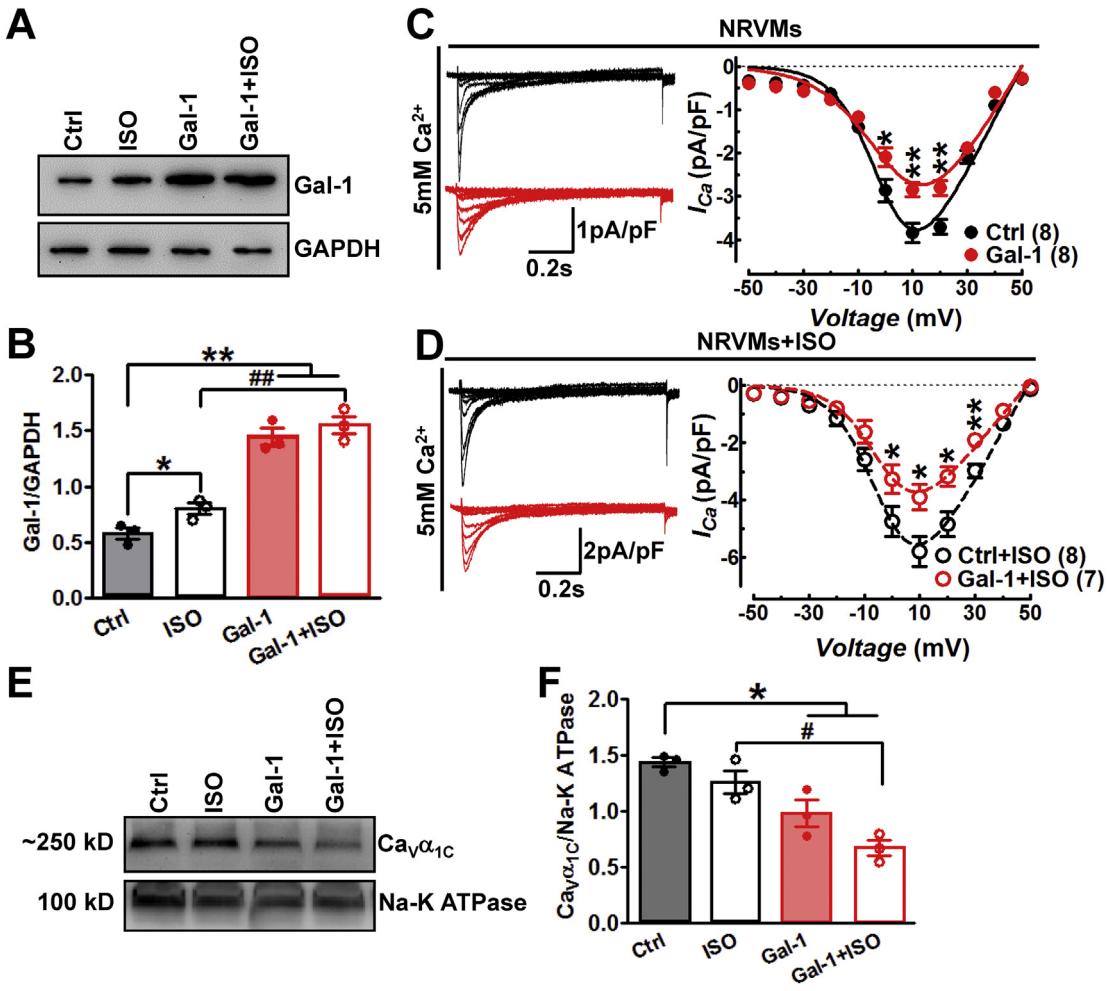

Fig. 2. Gal-1 inhibits the native $I_{Ca,L}$ and reduces the surface expression of $Ca_V1.2$ channels in NRVMs. (A) NRVMs were transfected with vector or Gal-1 expression plasmids upon the application with or without 1 μmol/L ISO, post 48 h transfection, immunoblotting was used to determine the expression of Gal-1 in NRVMs. GAPDH protein was detected as internal control. (B) The relative band densities were analyzed and normalized to GAPDH. The results were from three independent experiments. (C) Native $I_{Ca,L}$ was measured in the NRVMs transfected with vector (black) or Gal-1 (red) in 5 mmol/L Ca^{2+} bath solution. (D) $I_{Ca,L}$ of NRVMs transfected with vector (black) or Gal-1 (red) was also analyzed upon application with 1 μmol/L ISO. $^{*}P < 0.05$, $^{**}P < 0.01$ versus control, unpaired *t*-test. (E) NRVMs were transfected with vector or Gal-1 expression plasmids upon the application with or without 1 μmol/L ISO, post 48 h transfection, membrane proteins were extracted and immunoblotting was used to determine the surface expression of $Ca_V1.2$ α_{1C} in NRVMs. Na−K ATPase protein was detected as internal control. (F) The relative band densities were analyzed and normalized to Na−K ATPase. The results were from three independent experiments. $^{*}P < 0.05$, $^{**}P < 0.01$ versus control; $^{\#}P < 0.05$, $^{\#\#}P < 0.01$ versus ISO-treated NRVMs, one-way ANOVA followed by a Newman-Keuls method for post hoc pair-wise multiple comparisons.

affect the I_{Ba} or I_{Ca} of $Ca_V1.2_{CME9*}$ in transfected HEK293 cells when using 5 mmol/L Ba^{2+} (Fig. S4A) or 1.8 mmol/L Ca^{2+} (Fig. S4C) as charge carrier, respectively. However, it significantly decreased the currents of $Ca_V1.2_{CM\Delta E9*}$ channel in 5 mmol/L Ba^{2+} (Fig. S4B) or 1.8 mmol/L Ca^{2+} (Fig. S4D) bath solution, indicating Gal-1 specifically inhibits the currents of $Ca_V1.2_{CM\Delta E9*}$ channels in calcium-independent manner. However, Gal-1 did not significantly change the $Ca_V1.2_{CM\Delta E9*}$ channel gating properties, such as current-voltage relationship (Fig. S5A–B), steady-state activation (Fig. S5C–D) and steady-state inactivation (Fig. S5E–F).

To determine the mechanisms by which Gal-1 decreases $Ca_V1.2_{CM\Delta E9*}$ currents, we measured the ON-gating currents (Q_{ON}) reflecting the functional surface expression of $Ca_V1.2$ channels. It is found that Gal-1 had no effects on the $Ca_V1.2_{CME9*}$ channels (Fig. S4E), but it could significantly reduce the Q_{ON} of $Ca_V1.2_{CM\Delta E9*}$ channels (Fig. S4F), indicating Gal-1 inhibits the current of cardiac $Ca_V1.2_{\Delta E9*}$ channels by reducing the functional surface expression of $Ca_V1.2$ channels.

3.3. Overexpression of Gal-1 inhibits ISO or KCl-induced $[Ca^{2+}]_i$ elevation in NRVMs

We demonstrated that Gal-1 blunts the currents of $Ca_V1.2$ channels in NRVMs and HEK293 cells. This prompted us to investigate whether Gal-1 can modulate intracellular calcium homeostasis by restricting Ca^{2+} influx. To test this hypothesis, we monitored the real-time $[Ca^{2+}]_i$ under living cell station in NRVMs by using 4 μmol/L Fluo-4 AM as $[Ca^{2+}]_i$ indicator (Fig. 3A and C). ISO could bind and excite β-adrenergic receptors on the cardiomyocyte, in turn facilitates $Ca_V1.2$ channels, and subsequently increasing $[Ca^{2+}]_i$ [40]. Here, 10 μmol/L ISO was applied to NRVMs to trigger the elevation of $[Ca^{2+}]_i$, and this effect was almost blocked by co-incubating with 10 μmol/L $Ca_V1.2$ channel blocker diltiazem (DTZ) (Fig. 3B), indicating ISO-induced $[Ca^{2+}]_i$ elevation is actually mediated by $Ca_V1.2$ channels. However, overexpression of Gal-1 decreased elevated $[Ca^{2+}]_i$ induced by ISO as against vector-transfected NRVMs (Fig. 3B).

Unlike ISO-induced $[Ca^{2+}]_i$ elevation, the application of K^+ in extracellular solution could directly depolarize $Ca_V1.2$ channels to induce CICR. After ~5 min application with 60 mmol/L KCl, intracellular

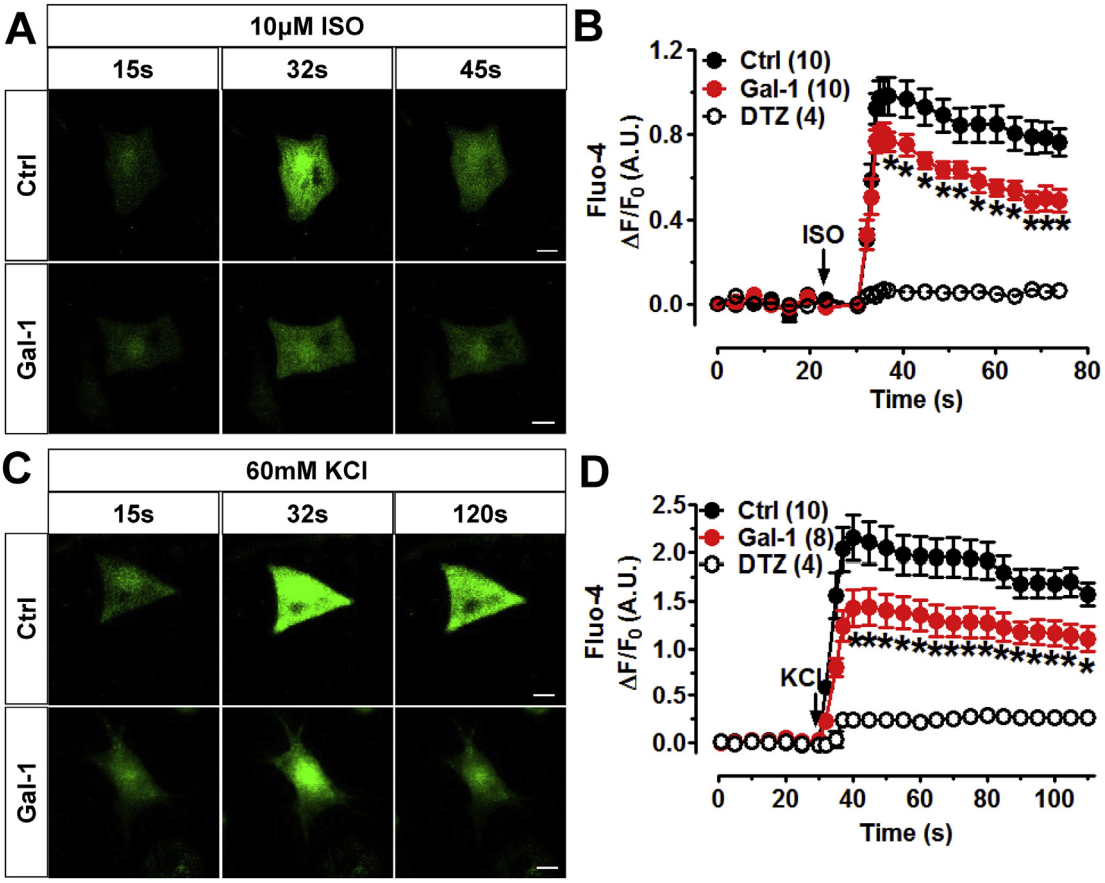

Fig. 3. Gal-1 inhibits ISO or KCl-induced $[Ca^{2+}]_i$ elevation in NRVMs. (A) 10 μmol/L ISO was applied in the bath solution of NRVMs transfected with vector or Gal-1 plasmids, real-time $[Ca^{2+}]_i$ was measured by Ca^{2+} fluorescence indicator Fluo-4 AM, and the fluorescent intensity was monitored by time series scanning mode under a confocal microscope. $\Delta[Ca^{2+}]_i$ fluorescence intensities were measured by dividing the changes in the fluorescent signal by the average resting fluorescence. (B) Plots of time course of fluorescent intensity after application with ISO in NRVMs transfected with vector (black) or Gal-1 plasmid (red), $\Delta[Ca^{2+}]_i$ was presented as $\Delta F/F_0$. (C) 60 mmol/L KCl was used to trigger $[Ca^{2+}]_i$ elevation of NRVMs transfected with vector or Gal-1 plasmids. (D) Plots of time course of fluorescent intensity after application with KCl in NRVMs transfected with vector (black) or Gal-1 plasmids (red). The $[Ca^{2+}]_i$ of NRVMs was also measured when co-incubating with 10 μmol/L $Ca_V1.2$ channel blocker diltiazem (DTZ) (black, empty circle). Scale bar: 20 μm. $^*P < 0.05$ versus control, unpaired *t*-test.

calcium increased to its maximal concentration, and co-incubation with DTZ also blocked this $[Ca^{2+}]_i$ elevation (Fig. 3D). Again, overexpression of Gal-1 decreased K^+-induced $[Ca^{2+}]_i$ elevation in NRVMs (Fig. 3D). These data strongly imply that Gal-1 could decrease $[Ca^{2+}]_i$ in cardiomyocyte, which is consistent with the idea that Gal-1 binds to the I-II loop of $Ca_V1.2$ calcium channel to inhibit its current [18]. However, neither ISO (Fig. S6A–B) nor KCl-induced $[Ca^{2+}]_i$ elevation (Fig. S6C–D) was potentiated after knockdown of Gal-1 in NRVMs, indicating that the efficacy of CICR might have reached to its maximum, which cannot further increase the $[Ca^{2+}]_i$ of NRVMs. Collectively, our data showed that Gal-1 could decrease ISO or KCl-induced $[Ca^{2+}]_i$ elevation in NRVMs, suggested to be mediated by the inhibition of $Ca_V1.2$ channel membrane expression and current.

3.4. Overexpression of Gal-1 attenuates ISO-induced cardiomyocyte hypertrophy

We next investigated whether Gal-1 can directly affect cardiomyocyte hypertrophy. NRVMs were transfected with Gal-1 expression plasmid or vector, after that ISO was applied to the cells. After 48 h ISO treatment in vector-transfected NRVMs, fetal genes' transcription, including *Nppa* (Fig. 4A), *Nppb* (Fig. 4B) and *Myh7* (Fig. 4C), was dramatically increased, and the cell surface area (Fig. 4D–E) and cell capacitance was enlarged (Fig. 4F). However, overexpression of Gal-1 could downregulate ISO-induced fetal genes' transcription in NRVMs (Fig. 4A–C). Moreover, it significantly reduced the cell surface area (Fig. 4D–E) and cell capacitance (Fig. 4F) of NRVMs treated with ISO. Knockdown of Gal-1 could potentiate ISO-induced *Nppb* (Fig. S7B) and *Myh7*'s (Fig. S7C) transcription, not *Nppa* (Fig. S7A), but it didn't significantly increase ISO-induced cell surface area (Fig. S7D–E) and cell capacitance (Fig. S7F) enlargement in NRVMs. Taken together, our data indicated that Gal-1 attenuates ISO-induced cardiomyocyte hypertrophy, which is thought to be mediated by the inhibition of $Ca_V1.2$ channel currents and decreased $[Ca^{2+}]_i$ in NRVMs.

3.5. Gal-1 inhibits ISO-induced phosphorylation of Ca^{2+}-dependent signaling proteins in NRVMs

We have investigated that Gal-1 could inhibit $[Ca^{2+}]_i$ of cardiomyocyte, and attenuate ISO-induced cardiomyocyte hypertrophy, but its signaling mechanisms are still unclear. CaMKII is known to play important roles in long-term stress-induced pathological cardiac hypertrophy [41]. Next, we investigated whether Gal-1 regulates intracellular calcium-dependent δCaMKII, the most abundant isoform expressed in cardiac muscles. NRVMs were stimulated by 10 μmol/L ISO treatment for 2 h, which gave a robust expression of phosphorylated δCaMKII (pδCaMKII^{Thr287}), not the total protein (Fig. 5A–B), as indicated by previous reports [42,43]. Increase of phosphorylated δCaMKII expression induced by ISO could be abolished by pretreatment with protein kinase A (PKA) inhibitor H89 or CaMKII inhibitor KN93, respectively (Fig. 5B). That indicated ISO-induced δCaMKII phosphorylation is mediated by cAMP-PKA signaling pathway. Furthermore, the

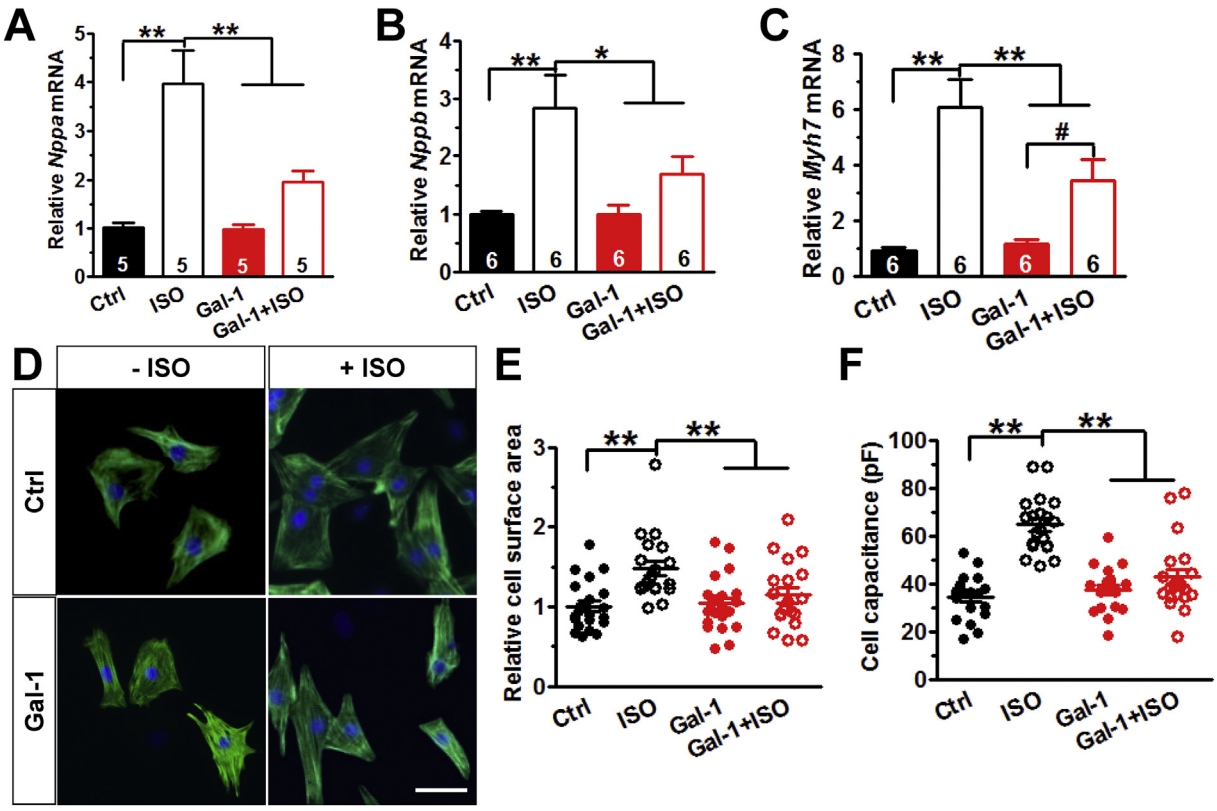

Fig. 4. Gal-1 inhibits fetal genes' transcription and reduces ISO-induced cell size enlargement in NRVMs. Rat *Nppa* (A), *Nppb* (B) and *Myh7* (C) mRNAs were determined by real-time RT-PCR in differentially-treated NRVMs, rat *Gapdh* mRNA was measured as internal control. The average data were from five or six separate experiments. (D) Representative images of NRVMs transfected with vector or Gal-1 plasmid after treatment with or without 1 μmol/L ISO for 48 h, immunofluorescence staining to determine cell surface area was carried out using anti-α-actinin antibody. Scale bar: 50 μm. (E) The analyzed cell surface areas were shown as scatter plots in differentially-treated NRVMs, control cells (n = 22), ISO-treated cells (n = 19), Gal-1 transfected cells (n = 22), and ISO-treated Gal-1 transfected cells (n = 19). (F) The cell capacitances were also analyzed as scatter plots in differentially-treated NRVMs. n = 20 cells each group. $^{*}P < 0.05$, $^{**}P < 0.01$ versus ISO-treated NRVMs, one-way ANOVA followed by a Newman-Keuls method for post hoc pair-wise multiple comparisons. $^{\#}P < 0.05$ versus Gal-1 transfected NRVMs, unpaired *t*-test.

phosphorylated HDAC4 (pHDAC4^{Ser632}) was also upregulated after ISO application (Fig. 5A and C). These observations suggested ISO upregulates fetal genes' transcription by phosphorylating δCaMKII and HDAC4. However, overexpression of Gal-1 reduced ISO-induced expression of phosphorylated δCaMKII (Fig. 5B) and HDAC4 (Fig. 5C) in NRVMs, indicating Gal-1 attenuates ISO-induced cardiomyocyte hypertrophy via δCaMKII-HDAC4 signaling pathway.

Further, we used LTCC agonist Bay K8644 to check the effect of Gal-1 on δCaMKII-HDAC4 signaling in NRVMs. Application with Bay K8644 could increase the phosphorylated expression of δCaMKII and HDAC4 in NRVMs (Fig. 5D–F), indicating activation of $Ca_V1.2$ channels indeed triggers these intracellular calcium-dependent signaling proteins. However, overexpression of Gal-1 could diminish Bay K8644-induced phosphorylation of δCaMKII (Fig. 5E) and HDAC4 (Fig. 5F) in NRVMs, respectively, suggesting that Gal-1 inhibits LTCC-δCaMKII-HDAC4 signaling, which represses the transcription of cardiac fetal genes and attenuates cardiomyocyte hypertrophy.

3.6. Gal-1 inhibits the ISO-triggered translocation of HDAC4 in NRVMs

It is well known that HDAC4 gets restricted to the cytoplasm instead of importing into the nucleus when phosphorylated upon activated δCaMKII, which relieves the depression of fetal genes' transcription [44,45]. Thus, we determined the translocation of HDAC4 in differentially-treated NRVMs. In non-treated NRVMs, the HDAC4 was mainly distributed at the surrounding of nucleus (Fig. 6), whereas HDAC4 staining was not restricted in nucleus instead of distributing in the cytosol of ISO-treated NRVMs (Fig. 6), indicating ISO could trigger the translocation of HDAC4 from nucleus to cytosol. However, HDAC4 remained to stay at the surrounding of nucleus of Gal-1-transfected and ISO-treated NRVMs (Fig. 6), suggesting Gal-1 could prevent the ISO-induced translocation of HDAC4 from nucleus to cytosol, thereby depresses the fetal genes' transcription and cardiomyocyte hypertrophy.

3.7. Increased expressions of $Ca_V1.2_{E9*}$ channels and Gal-1 in hypertrophic cardiomyocytes and hearts

In order to investigate the expression levels of Gal-1 and $Ca_V1.2_{E9*}$ channels in cardiomyocyte hypertrophy, rat NRVMs were treated with 1 μmol/L ISO. By using the primers to amplify and identify alternative exon 9* of $Ca_V1.2$ calcium channel, we found the proportion of $Ca_V1.2_{E9*}$ channels was increased by ~10% after 48 h ISO treatment in NRVMs (Fig. 7A–B). Unexpectedly, Gal-1 expression was also increased ~1.7-folds in ISO-treated NRVMs (Fig. 7A and C).

To address the pathological relevance, we used two different rat cardiac hypertrophic models, SHR and TAC-operated rats, to investigate the expressions of Gal-1 and $Ca_V1.2_{E9*}$ channels in hypertrophic hearts. Baseline characteristics indicated that the heart weight-to-body weight ratios were increased in SHR or TAC-operated rats as compared to age-matched WKY or sham-operated rats, respectively (Table S3). The M-mode echocardiography also indicated SHR (Table S4 and Fig. S8A–C) or TAC-operated rats (Table S5 and Fig. S8D–F) had an obvious cardiac hypertrophy, demonstrating IVS and LVPW thickness in diastole significantly increased.

Here, we observed the proportion of $Ca_V1.2_{E9*}$ channels were significantly increased in the ventricles of SHR (Fig. 7D–E) and TAC-

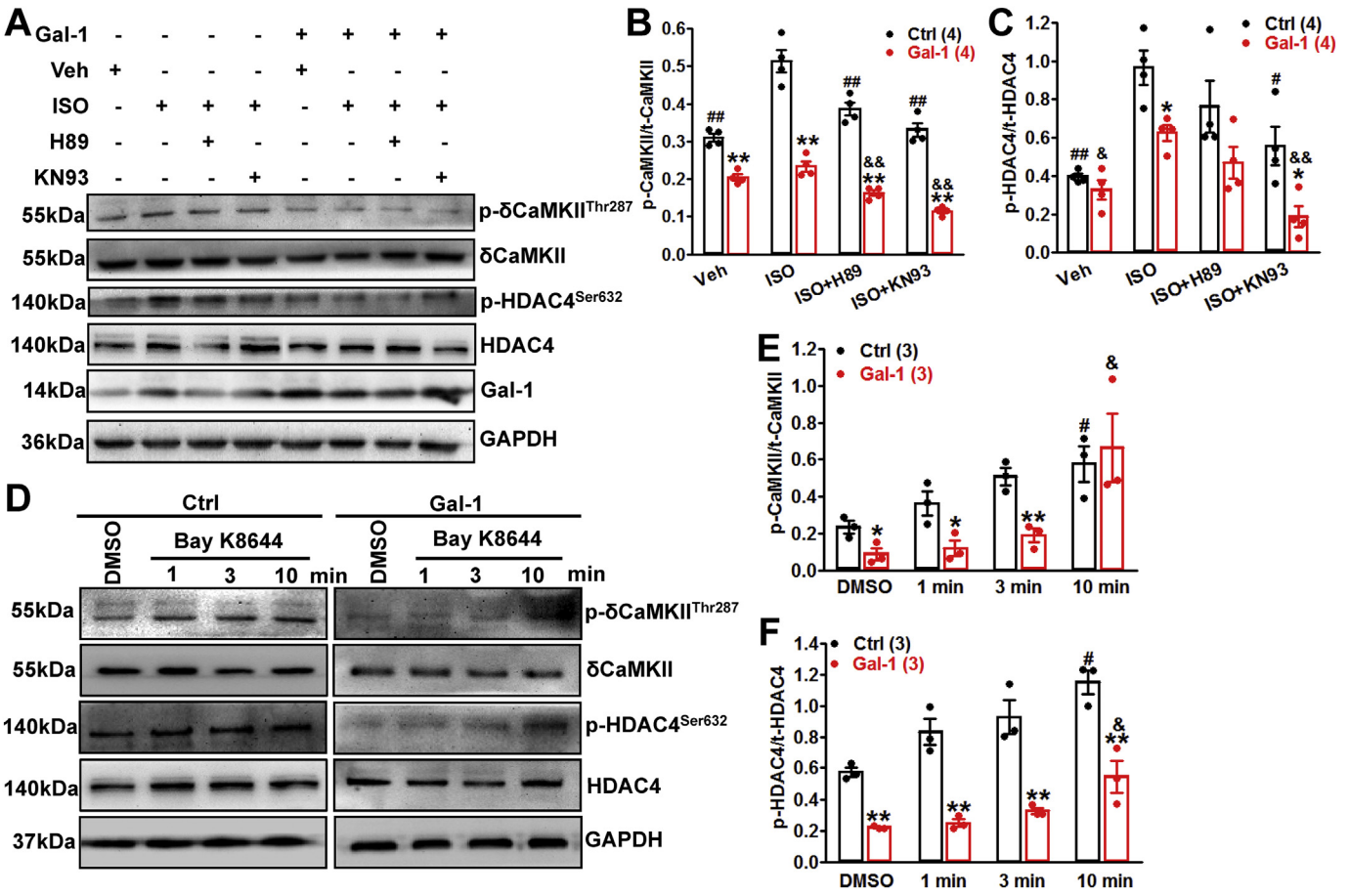

Fig. 5. Gal-1 inhibits the phosphorylation of δCaMKII and HDAC4 in NRVMs. (A) NRVMs were transfected with vector or Gal-1 plasmids, then cells were pretreated with 10 μmol/L PKA inhibitor H89 or 1 μmol/L CaMKII inhibitor KN93 for ~15 min before applying with 10 μmol/L ISO. The total protein from NRVMs was used to detect the expression of phosphorylated (p) or total (t) δCaMKII or HDAC4 by Western blotting, GAPDH protein was detected as internal control. The relative band densities were analyzed the expression of phosphorylated δCaMKII (B) or HDAC4 (C) in differentially-treated NRVMs. The results were from four independent experiments. $^{*}P < 0.05$, $^{**}P < 0.01$ versus control, unpaired *t*-test; $^{\#}P < 0.05$, $^{\#\#}P < 0.01$ versus ISO-treated vector-transfected NRVMs, $^{\&}P < 0.05$, $^{\&\&}P < 0.01$ versus ISO-treated Gal-1-transfected NRVMs, one-way ANOVA followed by a Newman-Keuls method for post hoc pair-wise multiple comparisons. (D) NRVMs were transfected with vector or Gal-1 plasmid, and treated with 5 μmol/L LTCC agonist Bay K8644, then cells were collected for detecting the expression of phosphorylated (p) or total (t) δCaMKII and HDAC4 by Western blotting at different timing points. The relative band densities were analyzed the expression of phosphorylated δCaMKII (E) or HDAC4 (F) in NRVMs. The results were from three independent experiments. $^{*}P < 0.05$, $^{**}P < 0.01$ versus control, unpaired *t*-test; $^{\#}P < 0.05$ versus DMSO-treated vector-transfected NRVMs, $^{\&}P < 0.05$ versus DMSO-treated Gal-1-transfected NRVMs, one-way ANOVA followed by a Newman-Keuls method for post hoc pair-wise multiple comparisons.

operated rats (Fig. 7H–I), which was in close agreement with previous report [46]. Moreover, expression of Gal-1 was also markedly increased in left ventricle from 20 weeks-old SHR (Fig. 7D and G) or TAC-operated rats (Fig. 7H and K) in contrast to age-matched WKY or sham-operated rats, which is similar with hypertrophic cardiomyocytes. However, the expressions of $Ca_V1.2$ α_{1C} subunits were dramatically decreased in left ventricle from 20 weeks-old SHR (Fig. 7D and F) or TAC-operated rats (Fig. 7H and J), which is also consistent with previous report [7].

4. Discussion

In addition to regulate the cardiac contractility, Ca^{2+} influx through $Ca_V1.2$ calcium channels modulates the intracellular signaling pathways and gene expression underlying cardiac hypertrophy and cardiomyopathies. As a hub, $Ca_V1.2$ calcium channel can be modulated by a series of mechanisms, including protein-protein interaction mediated by Gal-1 as reported previously [18]. In this study, we identified Gal-1 as a modulator of cardiac $Ca_V1.2$ calcium channel and provided evidence that Gal-1 attenuates ISO-induced cardiomyocyte hypertrophy via LTCC-δCaMKII-HDAC4 signaling pathway (Fig. 8A). Moreover, the aberrant expressions of Gal-1 and $Ca_V1.2$ with alternative exon 9* are found in cardiac hypertrophy (Fig. 8B), suggesting their potential roles in the development of cardiac hypertrophy.

$Ca_V\beta$ subunit is known to bind with α-interaction domain (AID) of I-II loop of $Ca_V1.2$ α_{1C} subunit to traffic it from endoplasmic reticulum (ER) to cell membrane, which affects the channel cell surface expression and gating [47]. Previous observations indicated that Gal-1 can bind to ER export motif of I-II loop of $Ca_V1.2$ channels, located behind AID domain, and the inclusion of alternative exon 9* prevents the binding between Gal-1 and $Ca_V1.2$ I-II loop. Functionally, Gal-1 inhibits the $I_{Ca,L}$ by decreasing the cell surface expression of $Ca_V1.2$ in VSMCs [18]. Mechanistically, the interaction between Gal-1 and $Ca_V1.2_{\Delta E9*}$ channel masks the AID domain to prevent the $Ca_V\beta$ subunit binding and trafficking of $Ca_V\alpha_{1C}$ subunit, results in the decreased $I_{Ca,L}$ [18,28]. In this study, we found Gal-1 could selectively reduce the $I_{Ca,L}$ of $Ca_V1.2_{CM\Delta E9*}$ channels in HEK293 cells. Compared to native $I_{Ca,L}$ in NRVMs, $I_{Ca,L}$ measured in HEK293 cells had a slower inactivation kinetics, which is attributed to the $Ca_V\beta_{2a}$ subunit anchoring to the cell membrane via its palmitoylation [48,49]. Noteworthy, in human ventricles, there are two major $Ca_V\beta$ subunits in the order of $\beta_{2b} > \beta_3 > \beta_{2a}$ [50,51], whether the inhibition of the cardiac $Ca_V1.2$

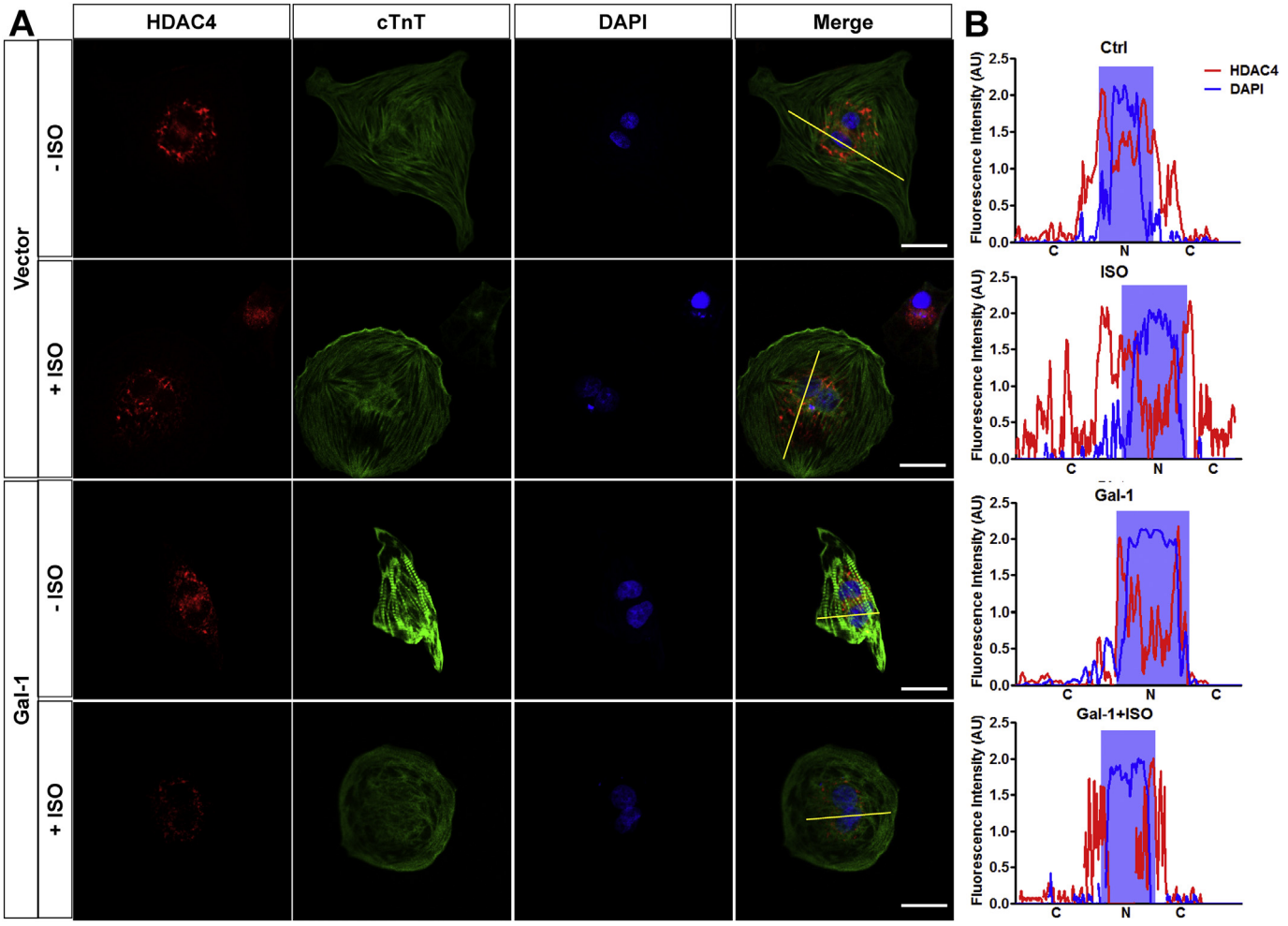

Fig. 6. Gal-1 prevents the ISO-triggered translocation of HDAC4 in NRVMs. (A) Immunofluorescence staining to determine the localization of HDAC4 in cardiomyocytes was carried out using anti-HDAC4 antibody (left panel, 1:100 dilution), cardiac troponin T (cTnT) staining (middle panel, 1:100 dilution) was used to label the cardiac myocytes, DAPI was used to label the nucleus, the right panel shows the merged image. Scale bar: 20 μm. (B) Fluorescence intensity profiles for HDAC4 (red) and DAPI (blue) along the yellow line drawn in the pictures, expressed as Arbitrary Unit (AU), in control (Ctrl), ISO-treated (ISO), Gal-1-transfected (Gal-1), or ISO-treated Gal-1-transfected (Gal-1 + ISO) NRVMs. Regions with high intensity of DAPI were considered as nucleus (N), the other regions were considered as cytosol (C).

channels by Gal-1 is dependent on the different $Ca_V\beta$ subunits warrants further investigation. Nevertheless, overexpression of Gal-1 decreased basal and ISO-induced $I_{Ca,L}$ of NRVMs, indicating that Gal-1 could directly inhibit the current of $Ca_V1.2$ channels in native cardiomyocyte by reducing the channel membrane expression.

In cardiomyocyte, Ca^{2+} influx through $Ca_V1.2$ channels triggers the activation of Ca^{2+} releasing channel ryanodine receptor 2 on the membrane of sarcoplasmic reticulum, inducing transient increase of $[Ca^{2+}]_i$ [52]. For the first time, we found that Gal-1 reduces ISO or KCl-induced elevation of $[Ca^{2+}]_i$ in cardiomyocytes. It is supposedly mediated by decreasing Ca^{2+} influx through $Ca_V1.2$ channels, owing to inhibition of $I_{Ca,L}$ by Gal-1. Overexpression of Gal-1 decreases only part of $[Ca^{2+}]_i$ could be explained by the part inhibition of $I_{Ca,L}$ by Gal-1 in NRVMs. Notably, overexpression of Gal-1 decreases the ISO-induced fetal genes' transcription, and diminishes ISO-induced cell size enlargement and cell capacitance increase, indicating Gal-1 attenuates ISO-induced cardiomyocyte hypertrophy via the inhibition of $[Ca^{2+}]_i$.

As the most abundantly expressed isoform in heart [41,53], δCaMKII is known to be regulated by $[Ca^{2+}]_i$ of cardiomyocyte [4]. Thus, the decrease of $[Ca^{2+}]_i$ by Gal-1 supposedly affects the phosphorylation of δCaMKII in cardiomyocyte. As expected, we found Gal-1 could inhibit the phosphorylation of δCaMKII in ISO or Bay K8644-treated cardiomyocytes. Owing to that $Ca_V1.2$ channel is also one of substrates of δCaMKII [54,55], reduced phosphorylation of δCaMKII might further decrease the activities of cardiac $Ca_V1.2$ channels. HDAC4, one of class II HDACs, is highly expressed in heart tissues [56], and it is known to be bound and phosphorylated by δCaMKII [45]. Treatment with δCaMKII inhibitor KN93 almost abolished ISO-induced HDAC4 phosphorylation as we demonstrated, suggesting that δCaMKII can affect cardiomyocyte hypertrophy via regulating the phosphorylation of HDAC4. Notably, Gal-1 could decrease ISO-induced phosphorylation and prevent translocation of HDAC4 in NRVMs, based on the inhibition of δCaMKII phosphorylation by Gal-1. Therefore, our data suggested that Gal-1 attenuates cardiomyocyte hypertrophy by inhibiting fetal genes' transcription, which is mediated by δCaMKII-HDAC4 signaling pathway.

In acute myocardial infarction, the expression of Gal-1 was increased in the infracted heart tissue [29]; moreover, the expression of Gal-1 could be induced by cardiac surgery [30]. Here, we found that the expression of Gal-1 was increased in the hypertrophic hearts induced by afterload pressure, suggesting that the upregulation of Gal-1 might be an important part of compensatory response in cardiac hypertrophy because they blunt β-adrenergic Ca^{2+} influx preventing runaway cardiomyocyte hypertrophy. $Ca_V1.2_{E9*}$ channels were rarely expressed in normal hearts (Fig. 1A and Fig. 7D and H), as indicated by previous reports [16,46]. However, we found the expression of $Ca_V1.2_{E9*}$

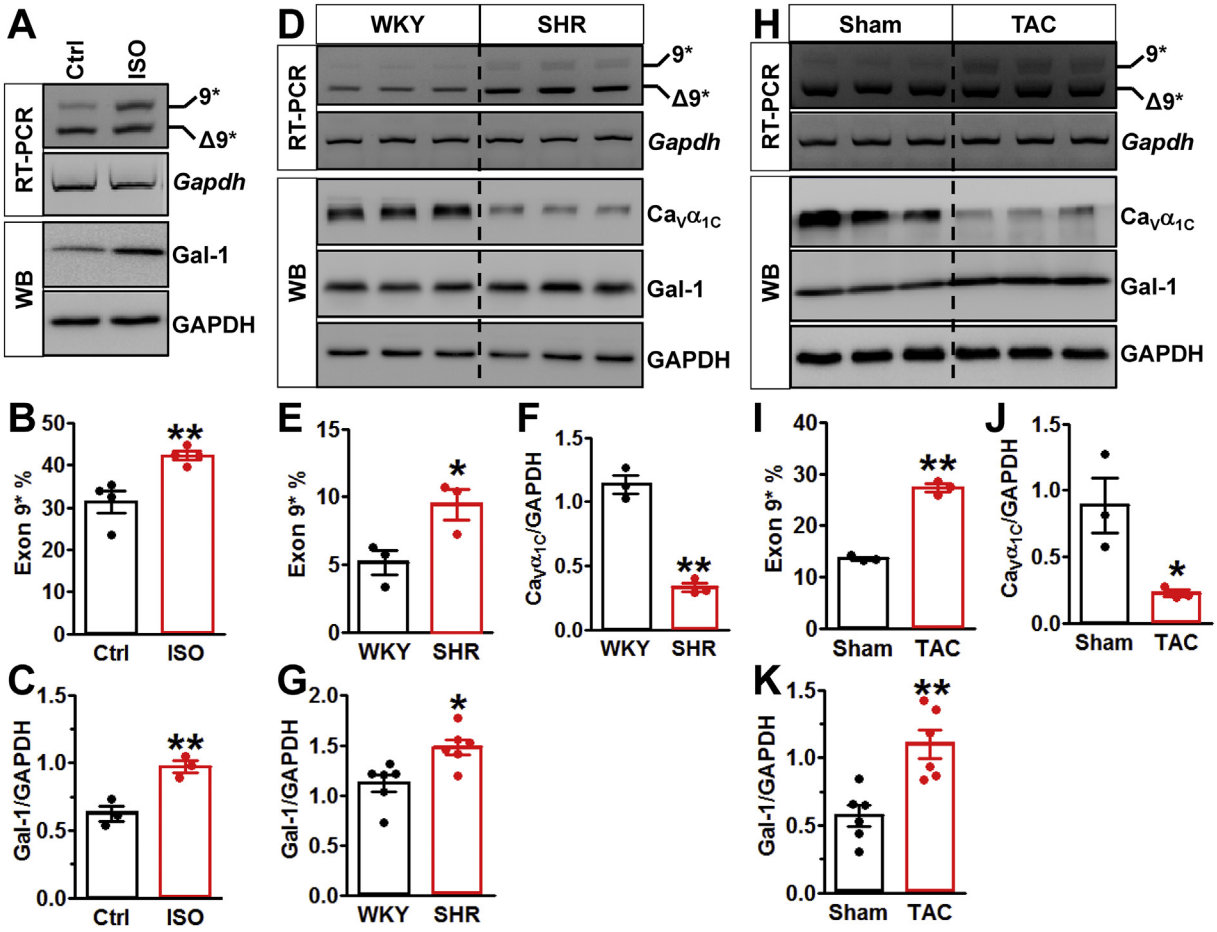

Fig. 7. The expressions of Gal-1 and $Ca_V1.2_{E9*}$ channels are upregulated in rat hypertrophic cardiomyocytes and hearts. (A) NRVMs were treated with 1 μmol/L isoproterenol (ISO) for 48 h to induce the hypertrophic phenotype. NRVMs were collected, $Ca_V1.2$ channels with or without exon 9* were determined by RT-PCR, the endogenous Gal-1 expression was detected by Western blotting. (B) The values for percent exon 9* inclusion were the upper band intensity divided by the summed intensities of upper and lower bands. (C) The relative expression of Gal-1 was normalized to GAPDH. The results were from 3 independent experiments. (D–G) $Ca_V1.2$ with or without exon 9* in hearts was detected by RT-PCR, *Gapdh* mRNA was detected as loading control. $Ca_V1.2$ α_{1C} and Gal-1 protein were measured in the lysate of left ventricle from 20-weeks-old WKY or SHR rats by Western blotting. n = 3–5 for WKY or SHR rats. (H–K) $Ca_V1.2_{E9*}$ and $Ca_V1.2_{\Delta E9*}$ channels of rats' heart were determined by RT-PCR, *Gapdh* mRNA was also detected as loading control. $Ca_V1.2$ α_{1C} and Gal-1 protein expression of left ventricle was measured in the rats post 14 days after sham (n = 3) or TAC surgery (n = 3–6) by Western blotting. $^*P < 0.05$, $^{**}P < 0.01$ versus control, age-matched WKY or sham-operated rats, unpaired *t*-test.

channels are increased in the hypertrophic cardiomyocytes and hearts. This observation was also found in myocardial infarction, which showed the expression of $Ca_V1.2_{\Delta E9*}$ channels were greatly reduced, whereas $Ca_V1.2_{E9*}$ channels were generated in the scar region of heart [20]. Though Gal-1 expression is upregulated in hypertrophic hearts, $Ca_V1.2_{E9*}$ channels are also increased, which might partly prevent the Gal-1's effects on cardiac $Ca_V1.2$ channels (Fig. 8B). This may explain why Gal-1 expression is increased, but the cardiac hypertrophy is still occurred. Therefore, we think overexpression of Gal-1 and simultaneous downregulation of $Ca_V1.2_{E9*}$ channels might produce a synergetic anti-hypertrophic action in the hearts.

Though we have explored the detailed molecular basis of Gal-1-$Ca_V1.2$ interaction in cardiomyocyte hypertrophy, this work still have some limitations. First, Gal-1 expression in neonatal cardiomyocyte is more than adult cardiomyocyte (Fig. S1). NRVM, used as a cell model, might not fully demonstrate the real pathological processes of adult cardiac hypertrophy. Second, Gal-1 expression plasmids are used and transfected into cardiomyocyte to induce the Gal-1 overexpression in the cells, which could be difficult to be applied in translational research, whether application with Gal-1 recombinant protein has the same effects on the cardiomyocyte hypertrophy is of value to be investigated. Third, the expressions of Gal-1 and $Ca_V1.2_{E9*}$ channels are dysregulated in rat hypertrophic hearts, suggesting the possible roles of Gal-1-$Ca_V1.2$ interaction in the development of cardiac hypertrophy. However, the in-vivo experiments are required to prove the consequent effects of Gal-1 on cardiac hypertrophy, which might be explored in future work.

Taken together, our study demonstrated that Gal-1 inhibits the $I_{Ca,L}$ of cardiac $Ca_V1.2_{\Delta E9*}$ channels by reducing the channel membrane expression, which decreases $[Ca^{2+}]_i$ of cardiomyocyte, downregulates δCaMKII-HDAC4 signaling, and prevents the translocation of HDAC4, with concomitant decrease in fetal genes' transcription and attenuation of cardiomyocyte hypertrophy. Significantly, the increased expression of Gal-1 in hypertrophic hearts suggests an important part of compensatory mechanism against cardiac hypertrophic remodeling.

Transparency document

The Transparency document associated this article can be found, in online version.

Acknowledgements

The authors would like to thank Professor Tuck Wah Soong

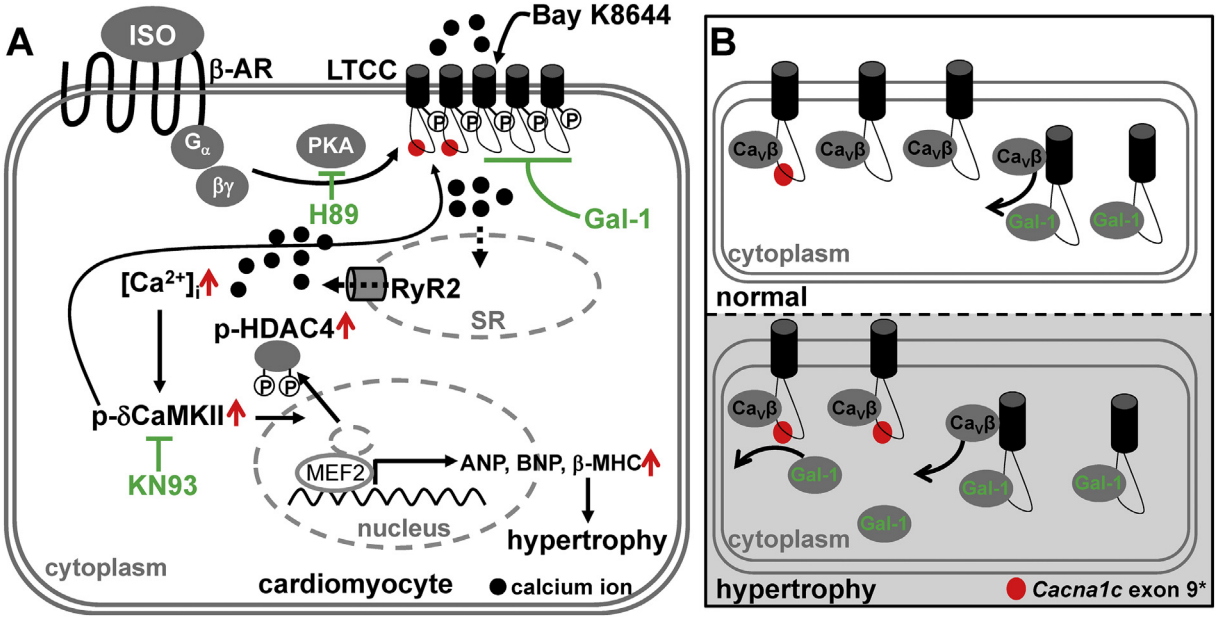

Fig. 8. Illustration of main findings in this study. (A) Working model of Gal-1 on the cardiomyocyte hypertrophy. Gal-1 inhibits the $I_{Ca,L}$ of $Ca_V1.2$ channels without alternative exon 9* ($Ca_V1.2_{\Delta E9*}$) by reducing the channel membrane expression, which will diminishes the intracellular Ca^{2+} concentration ($[Ca^{2+}]_i$) via calcium-induced calcium release mechanism. In turn, Gal-1 inhibits ISO-induced phosphorylation of δCaMKII and HDAC4, and prevents HDAC4 translocation from nucleus to cytosol, which depresses the fetal genes' transcription, and finally attenuates cardiomyocyte hypertrophy. (B) The possible mechanisms how Gal-1 interacts with $Ca_V1.2$ channels in cardiac hypertrophy. Gal-1 could compete with $Ca_V\beta$ subunits to bind with $Ca_V1.2_{\Delta E9*}$ channels, which induces the endoplasmic reticulum-associated protein degradation of $Ca_V1.2$ channels [28]. In normal hearts, Gal-1 and $Ca_V1.2$ channels with alternative exon 9* ($Ca_V1.2_{E9*}$) express in low level, which maintains a normal function of membrane $Ca_V1.2$ channels and homeostasis of $[Ca^{2+}]_i$ and intracellular calcium-dependent signaling. In hypertrophic hearts, Gal-1 expression is compensatory increased, it can bind with more $Ca_V1.2_{\Delta E9*}$ channels. However, $Ca_V1.2_{E9*}$ channels are still increased, which might prevent the Gal-1's effects on cardiac $Ca_V1.2$ channels and cardiac hypertrophy. β-AR, β-adrenergic receptor; MEF2, myocyte enhancer factor-2; RyR2, ryanodine receptor 2; SR, sarcoplasmic reticulum.

(Department of Physiology, Yong Loo Lin School of Medicine, National University of Singapore, Singapore) for kindly providing human $Ca_V1.2_{CM}$ and galectin-1 plasmids, and Professor Ling Chen (Department of Physiology, Nanjing Medical University, Nanjing, China) for the support of patch clamp set-up.

Funding

This work was supported by the National Natural Science Foundation of China (31371157, 81300193), the Natural Science Foundation of Jiangsu Province (BK20171482), the Natural Science Foundation for Young Scholars of Jiangsu Province (BK20130887), and a project funded by the Priority Academic Program Development of Jiangsu Higher Education Institutions (PAPD).

Disclosures

None.

Appendix A. Supplementary data

Supplementary data to this article can be found online at https://doi.org/10.1016/j.bbadis.2018.08.016.

References

[1] P. Palatini, S. Julius, The role of cardiac autonomic function in hypertension and cardiovascular disease, Curr. Hypertens. Rep. 11 (2009) 199–205.
[2] A. Mattiazzi, R.A. Bassani, A.L. Escobar, J. Palomeque, C.A. Valverde, M. Vila Petroff, D.M. Bers, Chasing cardiac physiology and pathology down the CaMKII cascade, Am. J. Physiol. Heart Circ. Physiol. 308 (2015) H1177–H1191.
[3] M.M. Kreusser, J. Backs, Integrated mechanisms of CaMKII-dependent ventricular remodeling, Front. Pharmacol. 5 (2014) 36.
[4] L.S. Maier, D.M. Bers, Role of Ca^{2+}/calmodulin-dependent protein kinase (CaMK) in excitation-contraction coupling in the heart, Cardiovasc. Res. 73 (2007) 631–640.
[5] X. Chen, H. Nakayama, X. Zhang, X. Ai, D.M. Harris, M. Tang, H. Zhang, C. Szeto, K. Stockbower, R.M. Berretta, A.D. Eckhart, W.J. Koch, J.D. Molkentin, S.R. Houser, Calcium influx through Cav1.2 is a proximal signal for pathological cardiomyocyte hypertrophy, J. Mol. Cell. Cardiol. 50 (2011) 460–470.
[6] S.A. Goonasekera, K. Hammer, M. Auger-Messier, I. Bodi, X. Chen, H. Zhang, S. Reiken, J.W. Elrod, R.N. Correll, A.J. York, M.A. Sargent, F. Hofmann, S. Moosmang, A.R. Marks, S.R. Houser, D.M. Bers, J.D. Molkentin, Decreased cardiac L-type Ca^{2+} channel activity induces hypertrophy and heart failure in mice, J. Clin. Invest. 122 (2012) 280–290.
[7] Z. Hu, J.W. Wang, D. Yu, J.L. Soon, D.P. de Kleijn, R. Foo, P. Liao, H.M. Colecraft, T.W. Soong, Aberrant splicing promotes proteasomal degradation of L-type $Ca_V1.2$ calcium channels by competitive binding for CaVbeta subunits in cardiac hypertrophy, Sci. Rep. 6 (2016) 35247.
[8] J. Wang, G. Li, D. Yu, Y.P. Wong, T.F. Yong, M.C. Liang, P. Liao, R. Foo, U.C. Hoppe, T.W. Soong, Characterization of $Ca_V1.2$ exon 33 heterozygous knockout mice and negative correlation between Rbfox1 and $Ca_V1.2$ exon 33 expressions in human heart failure, Channels 12 (2018) 51–57.
[9] I. Mahe, O. Chassany, A.S. Grenard, C. Caulin, J.F. Bergmann, Defining the role of calcium channel antagonists in heart failure due to systolic dysfunction, Am. J. Cardiovasc. Drugs 3 (2003) 33–41.
[10] C. Semsarian, I. Ahmad, M. Giewat, D. Georgakopoulos, J.P. Schmitt, B.K. McConnell, S. Reiken, U. Mende, A.R. Marks, D.A. Kass, C.E. Seidman, J.G. Seidman, The L-type calcium channel inhibitor diltiazem prevents cardiomyopathy in a mouse model, J. Clin. Invest. 109 (2002) 1013–1020.
[11] Y. Liao, M. Asakura, S. Takashima, A. Ogai, Y. Asano, H. Asanuma, T. Minamino, H. Tomoike, M. Hori, M. Kitakaze, Benidipine, a long-acting calcium channel blocker, inhibits cardiac remodeling in pressure-overloaded mice, Cardiovasc. Res. 65 (2005) 879–888.
[12] Z.Z. Tang, M.C. Liang, S. Lu, D. Yu, C.Y. Yu, D.T. Yue, T.W. Soong, Transcript scanning reveals novel and extensive splice variations in human l-type voltage-gated calcium channel, Cav1.2 alpha1 subunit, J. Biol. Chem. 279 (2004) 44335–44343.
[13] P. Liao, T.F. Yong, M.C. Liang, D.T. Yue, T.W. Soong, Splicing for alternative structures of Cav1.2 Ca^{2+} channels in cardiac and smooth muscles, Cardiovasc. Res. 68 (2005) 197–203.
[14] X. Cheng, J. Pachuau, E. Blaskova, M. Asuncion-Chin, J. Liu, A.M. Dopico, J.H. Jaggar, Alternative splicing of Cav1.2 channel exons in smooth muscle cells of resistance-size arteries generates currents with unique electrophysiological properties, Am. J. Physiol. Heart Circ. Physiol. 297 (2009) H680–H688.
[15] P. Liao, D. Yu, G. Li, T.F. Yong, J.L. Soon, Y.L. Chua, T.W. Soong, A smooth muscle

Cav1.2 calcium channel splice variant underlies hyperpolarized window current and enhanced state-dependent inhibition by nifedipine, J. Biol. Chem. 282 (2007) 35133–35142.
[16] P. Liao, D. Yu, S. Lu, Z. Tang, M.C. Liang, S. Zeng, W. Lin, T.W. Soong, Smooth muscle-selective alternatively spliced exon generates functional variation in Cav1.2 calcium channels, J. Biol. Chem. 279 (2004) 50329–50335.
[17] M.A. Nystoriak, K. Murakami, P.L. Penar, G.C. Wellman, $Ca_V1.2$ splice variant with exon 9* is critical for regulation of cerebral artery diameter, Am. J. Physiol. Heart Circ. Physiol. 297 (2009) H1820–H1828.
[18] J. Wang, S.S. Thio, S.S. Yang, D. Yu, C.Y. Yu, Y.P. Wong, P. Liao, S. Li, T.W. Soong, Splice variant specific modulation of $Ca_V1.2$ calcium channel by galectin-1 regulates arterial constriction, Circ. Res. 109 (2011) 1250–1258.
[19] R.H. Cox, S. Fromme, Expression of calcium channel subunit variants in small mesenteric arteries of WKY and SHR, Am. J. Hypertens. 28 (2015) 1229–1239.
[20] P. Liao, G. Li, D.J. Yu, T.F. Yong, J.J. Wang, J. Wang, T.W. Soong, Molecular alteration of $Ca_V1.2$ calcium channel in chronic myocardial infarction, Pflugers Arch. 458 (2009) 701–711.
[21] S. Tiwari, Y. Zhang, J. Heller, D.R. Abernethy, N.M. Soldatov, Atherosclerosis-related molecular alteration of the human $Ca_V1.2$ calcium channel alpha1C subunit, Proc. Natl. Acad. Sci. U. S. A. 103 (2006) 17024–17029.
[22] Y. Zhou, J. Fan, H. Zhu, L. Ji, W. Fan, I. Kapoor, Y. Wang, Y. Wang, G. Zhu, J. Wang, Aberrant splicing induced by dysregulated Rbfox2 produces enhanced function of $Ca_V1.2$ calcium channel and vascular myogenic tone in hypertension, Hypertension 70 (2017) 1183–1192.
[23] S.H. Barondes, V. Castronovo, D.N. Cooper, R.D. Cummings, K. Drickamer, T. Feizi, M.A. Gitt, J. Hirabayashi, C. Hughes, K. Kasai, et al., Galectins: a family of animal beta-galactoside-binding lectins, Cell 76 (1994) 597–598.
[24] N.W. van der Hoeven, M.R. Hollander, C. Yildirim, M.F. Jansen, P.F. Teunissen, A.J. Horrevoets, T.C. van der Pouw Kraan, N. van Royen, The emerging role of galectins in cardiovascular disease, Vasc. Pharmacol. 81 (2016) 31–41.
[25] I. Camby, M. Le Mercier, F. Lefranc, R. Kiss, Galectin-1: a small protein with major functions, Glycobiology 16 (2006) 137R–157R.
[26] J.M. Cousin, M.J. Cloninger, The role of galectin-1 in cancer progression, and synthetic multivalent systems for the study of galectin-1, Int. J. Mol. Sci. 17 (2016).
[27] E.P. Moiseeva, Q. Javed, E.L. Spring, D.P. de Bono, Galectin 1 is involved in vascular smooth muscle cell proliferation, Cardiovasc. Res. 45 (2000) 493–502.
[28] Z. Hu, G. Li, J.W. Wang, S.Y. Chong, D. Yu, X. Wang, J.L. Soon, M.C. Liang, Y.P. Wong, N. Huang, H.M. Colecraft, P. Liao, T.W. Soong, Regulation of blood pressure by targeting $Ca_V1.2$-galectin-1 protein interaction, Circulation (2018), https://doi.org/10.1161/CIRCULATIONAHA.117.031231.
[29] I.M. Seropian, J.P. Cerliani, S. Toldo, B.W. Van Tassell, J.M. Ilarregui, G.E. Gonzalez, M. Matoso, F.N. Salloum, R. Melchior, R.J. Gelpi, J.C. Stupirski, A. Benatar, K.A. Gomez, C. Morales, A. Abbate, G.A. Rabinovich, Galectin-1 controls cardiac inflammation and ventricular remodeling during acute myocardial infarction, Am. J. Pathol. 182 (2013) 29–40.
[30] S. Al-Salam, S. Hashmi, Galectin-1 in early acute myocardial infarction, PLoS One 9 (2014) e86994.
[31] M. Shimano, N. Ouchi, K. Nakamura, Y. Oshima, A. Higuchi, D.R. Pimentel, K.D. Panse, E. Lara-Pezzi, S.J. Lee, F. Sam, K. Walsh, Cardiac myocyte-specific ablation of follistatin-like 3 attenuates stress-induced myocardial hypertrophy, J. Biol. Chem. 286 (2011) 9840–9848.
[32] J.S. Hulot, J. Fauconnier, D. Ramanujam, A. Chaanine, F. Aubart, Y. Sassi, S. Merkle, O. Cazorla, A. Ouille, M. Dupuis, L. Hadri, D. Jeong, S. Muhlstedt, J. Schmitt, A. Braun, L. Benard, Y. Saliba, B. Laggerbauer, B. Nieswandt, A. Lacampagne, R.J. Hajjar, A.M. Lompre, S. Engelhardt, Critical role for stromal interaction molecule 1 in cardiac hypertrophy, Circulation 124 (2011) 796–805.
[33] X. Zhu, J. Fang, J. Gong, J.H. Guo, G.N. Zhao, Y.X. Ji, H.Y. Liu, X. Wei, H. Li, Cardiac-specific EPI64C blunts pressure overload-induced cardiac hypertrophy, Hypertension 67 (2016) 866–877.
[34] Z. Kassiri, C. Zobel, T.T. Nguyen, J.D. Molkentin, P.H. Backx, Reduction of I(to) causes hypertrophy in neonatal rat ventricular myocytes, Circ. Res. 90 (2002) 578–585.
[35] S.G. Kaufmann, R.E. Westenbroek, C. Zechner, A.H. Maass, S. Bischoff, J. Muck, E. Wischmeyer, T. Scheuer, S.K. Maier, Functional protein expression of multiple sodium channel alpha- and beta-subunit isoforms in neonatal cardiomyocytes, J. Mol. Cell. Cardiol. 48 (2010) 261–269.
[36] S. Clouet, L. Di Pietrantonio, E.P. Daskalopoulos, H. Esfahani, M. Horckmans, M. Vanorle, A. Lemaire, J.L. Balligand, C. Beauloye, J.M. Boeynaems, D. Communi, Loss of mouse P2Y6 nucleotide receptor is associated with physiological macrocardia and amplified pathological cardiac hypertrophy, J. Biol. Chem. 291 (2016) 15841–15852.
[37] L. Ji, H. Zhu, H. Chen, W. Fan, J. Chen, J. Chen, G. Zhu, J. Wang, Modulation of $Ca_V1.2$ calcium channel by neuropeptide W regulates vascular myogenic tone via G protein-coupled receptor 7, J. Hypertens. 33 (2015) 2431–2442.
[38] F. Hohendanner, S. Ljubojevic, N. MacQuaide, M. Sacherer, S. Sedej, L. Biesmans, P. Wakula, D. Platzer, S. Sokolow, A. Herchuelz, G. Antoons, K. Sipido, B. Pieske, F.R. Heinzel, Intracellular dyssynchrony of diastolic cytosolic $[Ca^{2+}]$ decay in ventricular cardiomyocytes in cardiac remodeling and human heart failure, Circ. Res. 113 (2013) 527–538.
[39] R.M. Paredes, J.C. Etzler, L.T. Watts, W. Zheng, J.D. Lechleiter, Chemical calcium indicators, Methods 46 (2008) 143–151.
[40] W.A. Catterall, Regulation of cardiac calcium channels in the fight-or-flight response, Curr. Mol. Pharmacol. 8 (2015) 12–21.
[41] J. Backs, T. Backs, S. Neef, M.M. Kreusser, L.H. Lehmann, D.M. Patrick, C.E. Grueter, X. Qi, J.A. Richardson, J.A. Hill, H.A. Katus, R. Bassel-Duby, L.S. Maier, E.N. Olson, The delta isoform of CaM kinase II is required for pathological cardiac hypertrophy and remodeling after pressure overload, Proc. Natl. Acad. Sci. U. S. A. 106 (2009) 2342–2347.
[42] A. Ishida, H. Fujisawa, Stabilization of calmodulin-dependent protein kinase II through the autoinhibitory domain, J. Biol. Chem. 270 (1995) 2163–2170.
[43] H. Ma, R.D. Groth, S.M. Cohen, J.F. Emery, B. Li, E. Hoedt, G. Zhang, T.A. Neubert, R.W. Tsien, gammaCaMKII shuttles Ca^{2+}/CaM to the nucleus to trigger CREB phosphorylation and gene expression, Cell 159 (2014) 281–294.
[44] M. Hohl, M. Wagner, J.C. Reil, S.A. Muller, M. Tauchnitz, A.M. Zimmer, L.H. Lehmann, G. Thiel, M. Bohm, J. Backs, C. Maack, HDAC4 controls histone methylation in response to elevated cardiac load, J. Clin. Invest. 123 (2013) 1359–1370.
[45] J. Backs, K. Song, S. Bezprozvannaya, S. Chang, E.N. Olson, CaM kinase II selectively signals to histone deacetylase 4 during cardiomyocyte hypertrophy, J. Clin. Invest. 116 (2006) 1853–1864.
[46] Z.Z. Tang, P. Liao, G. Li, F.L. Jiang, D. Yu, X. Hong, T.F. Yong, G. Tan, S. Lu, J. Wang, T.W. Soong, Differential splicing patterns of L-type calcium channel Cav1.2 subunit in hearts of spontaneously hypertensive rats and Wistar Kyoto rats, Biochim. Biophys. Acta 1783 (2008) 118–130.
[47] M. Pragnell, M. De Waard, Y. Mori, T. Tanabe, T.P. Snutch, K.P. Campbell, Calcium channel beta-subunit binds to a conserved motif in the I-II cytoplasmic linker of the alpha 1-subunit, Nature 368 (1994) 67–70.
[48] A.J. Chien, K.M. Carr, R.E. Shirokov, E. Rios, M.M. Hosey, Identification of palmitoylation sites within the L-type calcium channel beta2a subunit and effects on channel function, J. Biol. Chem. 271 (1996) 26465–26468.
[49] N. Qin, D. Platano, R. Olcese, J.L. Costantin, E. Stefani, L. Birnbaumer, Unique regulatory properties of the type 2a Ca^{2+} channel beta subunit caused by palmitoylation, Proc. Natl. Acad. Sci. U. S. A. 95 (1998) 4690–4695.
[50] R. Hullin, I.F. Khan, S. Wirtz, P. Mohacsi, G. Varadi, A. Schwartz, S. Herzig, Cardiac L-type calcium channel beta-subunits expressed in human heart have differential effects on single channel characteristics, J. Biol. Chem. 278 (2003) 21623–21630.
[51] H.M. Colecraft, B. Alseikhan, S.X. Takahashi, D. Chaudhuri, S. Mittman, V. Yegnasubramanian, R.S. Alvania, D.C. Johns, E. Marban, D.T. Yue, Novel functional properties of Ca^{2+} channel beta subunits revealed by their expression in adult rat heart cells, J. Physiol. 541 (2002) 435–452.
[52] A.R. Marks, Cardiac intracellular calcium release channels: role in heart failure, Circ. Res. 87 (2000) 8–11.
[53] L.S. Maier, T. Zhang, L. Chen, J. DeSantiago, J.H. Brown, D.M. Bers, Transgenic CaMKIIdeltaC overexpression uniquely alters cardiac myocyte Ca^{2+} handling: reduced SR Ca^{2+} load and activated SR Ca^{2+} release, Circ. Res. 92 (2003) 904–911.
[54] T.S. Lee, R. Karl, S. Moosmang, P. Lenhardt, N. Klugbauer, F. Hofmann, T. Kleppisch, A. Welling, Calmodulin kinase II is involved in voltage-dependent facilitation of the L-type Cav1.2 calcium channel: identification of the phosphorylation sites, J. Biol. Chem. 281 (2006) 25560–25567.
[55] A. Blaich, A. Welling, S. Fischer, J.W. Wegener, K. Kostner, F. Hofmann, S. Moosmang, Facilitation of murine cardiac L-type $Ca_V1.2$ channel is modulated by calmodulin kinase II-dependent phosphorylation of S1512 and S1570, Proc. Natl. Acad. Sci. U. S. A. 107 (2010) 10285–10289.
[56] J. Backs, E.N. Olson, Control of cardiac growth by histone acetylation/deacetylation, Circ. Res. 98 (2006) 15–24.